Nanoscale

Structurally Colored Protease Responsive Nanoparticle Hydrogels with Degradation-Directed Assembly

Journal:	*Nanoscale*
Manuscript ID	NR-ART-05-2019-004624.R1
Article Type:	Paper
Date Submitted by the Author:	05-Aug-2019
Complete List of Authors:	Torres Jr, Leopoldo ; University of Maryland at College Park, Fischell Department of Bioengineering Daristotle, John ; University of Maryland at College Park, Fischell Department of Bioengineering Ayyub, Omar ; University of Maryland at College Park, Chemical and Biomolecular Engineering Bellato Meinhardt, Bianca; University of Maryland at College Park, Chemical and Biomolecular Engineering Margaronis, Artemis ; University of Maryland at College Park, Chemical and Biomolecular Engineering Garimella, Havisha ; University of Maryland at College Park, Fischell Department of Bioengineering Seifert, Sönke; Argonne National Laboratory, X-ray Science Division Bedford, Nicholas; University of New South Wales Faculty of Engineering Woehl, Taylor; University of Maryland, Chemical and Biomolecular Engineering Kofinas, Peter; University of Maryland at College Park, Chemical and Biomolecular Engineering

ARTICLE

Structurally Colored Protease Responsive Nanoparticle Hydrogels with Degradation-Directed Assembly

Received 00th January 20xx,
Accepted 00th January 20xx

DOI: 10.1039/x0xx00000x

Leopoldo Torres Jr,[a] John L. Daristotle, [a] Omar B. Ayyub, [b] Bianca M. Bellato Meinhardt, [b] Havisha Garimella,[a] Artemis Margaronis,[b] Soenke Seifert,[c] Nicholas Bedford,[d] Taylor J. Woehl,[b] and Peter Kofinas *[b]

A tunable protease responsive nanoparticle hydrogel (PRNH) that demonstrates large non-iridescent color changes due to a degradation-directed assembly of nanoparticles is reported. Structurally colored composites are fabricated with silica particles, 4-arm poly(ethylene glycol) norbornene (4PEGN), and a proteolytically degradable peptide. When placed in a protease solution, the peptide crosslinks degrade causing electrostatic binding and adsorption of the polymer to the particle surface which leads to the assembly of particles into compact amorphous arrays with structural color. The particle surface charge and size is investigated to probe their effect on the assembly mechanism. Interestingly, only PRNHs with highly negative particle surface charge exhibit color changes after degradation. Ultra-small angle x-ray scattering revealed that the particles become coated in polymer after degradation, producing a material with less order compared to the initial state. Altering the particle diameter modulates the composites' color, and all sizes investigated (178–297 nm) undergo the degradation-directed assembly. Varying the amount of 4PEGN adjusts the swollen PRNH color and has no effect on the degradation-directed assembly. Taken together, the effects of surface charge, particle size, and polymer concentration allow for the formulation of new design rules for fabricating tunable PRNHs that display vivid changes in structural color upon degradation.

Introduction

Nanoparticle-hydrogel composites that exhibit structural color have gained interest due to their ability to alter their interparticle distance and change color in response to chemical, biological, or physical stimuli.[1] For this reason, particle assembly strategies to fabricate functional structurally colored materials have been widely investigated. These methods have also been applied to the fabrication of synthetic opals,[2] ink-based printing,[3] coloration by spray coating,[4] and design of well-ordered materials as optical waveguides.[5,6] Generally, particle assembly processes employ a range of physical interactions such as capillary action,[7] gravity assisted sedimentation,[8] evaporation,[9] and electric[10] or magnetic field[11] alignment to provide attractive forces between particles in a suspension. In addition to attractive forces, long-range periodic close-packed structures require repulsive forces, such as electrostatic repulsion or steric hindrance, to prevent particle aggregation and produce an energetically favorable equilibrium interparticle-distance.[12]

Nanoparticle assemblies exhibiting structural color can be entrapped in a hydrogel network that preserves their architecture and color upon *in situ* polymerization and crosslinking of monomers. We refer to these types of materials as structurally colored composites (SCC). The SCC will change color according to the degree of swelling or collapse of the hydrogel matrix[13] since the wavelength of light diffracted is proportional to the center-to-center distance of the nanoparticles.[14] Typically, large color changes can be obtained only through high concentration of charged functional groups on the polymer[15] because the network swells to balance the charged functional groups within the matrix .[16] In this work, color modulation is enabled by the degradation of the hydrogel network which directs the reassembly of the nanoparticles into a new, energetically stable periodic arrangement that diffracts a different wavelength of visible light.

Here we investigate a protease responsive nanoparticle hydrogel (PRNH) composed of highly charged silica particles embedded within a dicysteine peptide and poly(ethylene glycol) hydrogel that undergoes a boolean-like color change due to controlled particle aggregation caused by the proteolytic degradation of the synthetic peptide monomer. Instead of swelling or de-swelling in response to charged

---

[a] *Fischell Department of Bioengineering†, University of Maryland, Room 3102 A. James Clark Hall, 8278 Paint Branch Dr., College Park, MD 20742, USA.*
[b] *Department of Chemical and Biomolecular Engineering‡, University of Maryland, 4418 Stadium Dr., College Park, MD 20742, USA.*
E-mail:kofinas@umd.edu
[c] *X-Ray Sciences Division, Argonne National Laboratory, Argonne, IL 60439, USA.*
[d] *School of Chemical Engineering, University of New South Wales, Hill Street, Sydney, NSW 2052, Australia.*

Electronic Supplementary Information (ESI) available: [details of any supplementary information available should be included here]. See DOI: 10.1039/x0xx00000x

functional groups in the hydrogel matrix, aggregation is triggered by the adsorption of degraded hydrogel fragments onto the surface of silica particles, which occurs due to an increase in particle mobility facilitated by the degrading hydrogel network. The PRNH is fabricated by *in situ* polymerization of a centrifuged mixture of suspended particles and thiol-ene reactive monomers. A limitation of conventional approaches to producing SCCs is colloid instability during assembly due to attractive interactions between the monomers and particles. Centrifugation allows for the PRNH to have order—and therefore structural color—both before and after the degradation-directed assembly event.

This manuscript identifies critical parameters such as particle size, particle charge, and polymer concentration that affect changes in the interparticle spacing before and after degradation of the hydrogel. We fabricated PRNHs displaying several structural colors to determine whether the particle assembly mechanism was dependent on particle size or polymer concentration. In addition, PRNHs with particles of varying surface charges were fabricated to determine whether the particle assembly was sensitive to the sign or magnitude of particle surface charge. Probe reflectance spectroscopy was used to measure the color of the PRNH before and after degradation. The PRNH microstructure was characterized by ultra-small angle x-ray scattering (USAXS) and scanning electron microscopy (SEM). Our results reveal general design rules for tunable PRNHs. First, if the surface charge of silica particles is sufficiently high, protease-induced degradation and assembly will result in a blue-shift in structural color. If the first design rule is satisfied, the starting color and the degree of the color shift upon degradation are determined by the particle size and polymer concentration, respectively. In other words, polymer concentration and particle size can be used to independently tune the swollen and degraded color to achieve rationally tunable PRNHs.

Results and Discussion

Protease Responsive Nanoparticle Hydrogel Fabrication

The structurally colored PRNH is composed of nearly monodisperse silica particles, a 10 kDa 4-arm poly(ethylene glycol) terminated with norbornene (4PEGN) crosslinker, UV photoinitiator, and a dicysteine peptide, CY↓KC, bifunctional monomer. These components undergo a three-step fabrication process in which they are centrifuged, sandwich-casted between two glass slides, and subsequently irradiated with UV light to polymerize the 4PEGN and CY↓KC (Figure 1A and 1B). The first step, centrifugation, sediments the particles and in conjunction with electrostatic repulsion form a close-packed periodic microstructure surrounded by monomers (Figure 1Bi and 1Bii). The centrifuged mixture exhibits structural color because the silica particles assemble in a periodic structure of the same size scale as visible light, and the incident light can constructively interfere with the structure.[17] The second step, compressing the particle and monomer pellet, produces a film that is uniform in thickness (250 μm) (Figure 1Biii). The particle arrays in the film are isotropic, have short-range order, and have a broad distribution of interparticle spacing.[18] These structure properties give rise to broad reflectance peaks and angle-independent structural color. [19,20] The diffracted peak wavelength is not significantly altered by the concentration of particles within the suspension (Figure S1), but concentrations

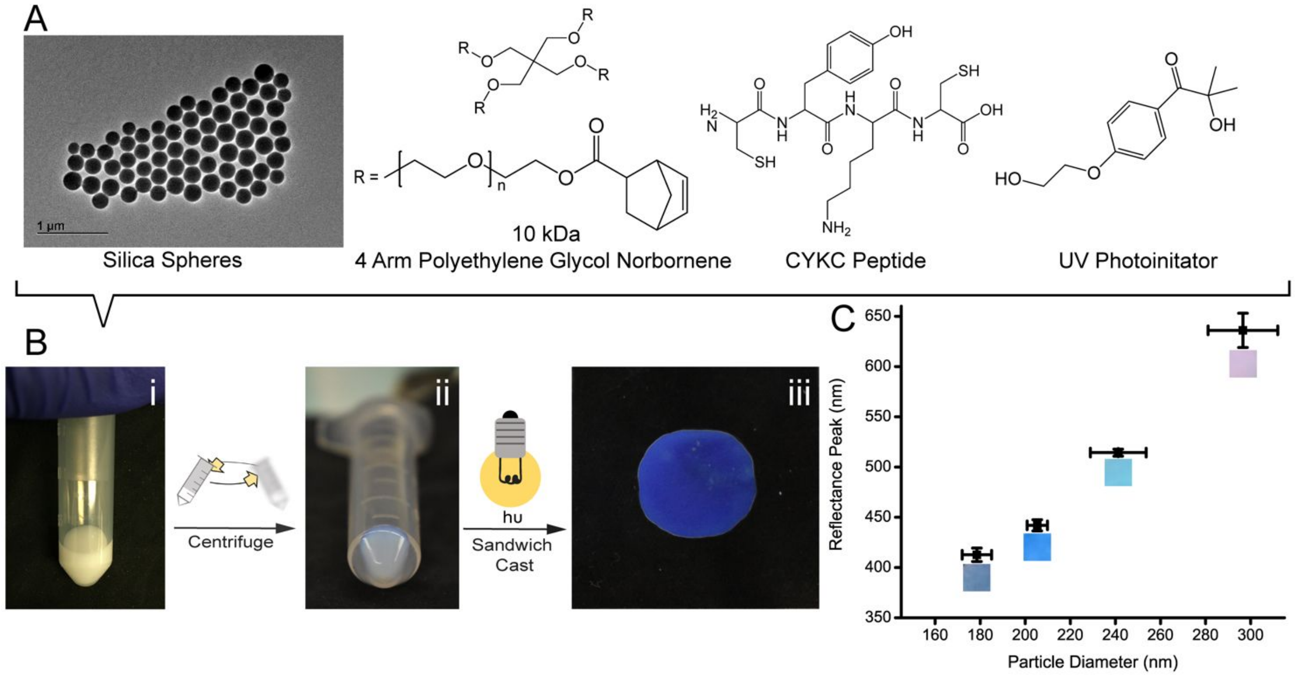

Fig. 1 Fabrication of angle-independent structurally colored particle hydrogel composites. (A) The components of the protease responsive nanoparticle hydrogel. (Bi) 205 nm silica particles were suspended in a solution of 4PEGN, CY↓KC, and photoinitiator. (Bii) A blue pellet was produced by centrifuging the components at 19k times the gravitational acceleration for 2.5 minutes. (Biii) The pellet was sandwich cast between two glass slides to produce a thin film and irradiated with UV to undergo thiol-ene click chemistry. (C) The peak wavelengths diffracted by 15% 4PEGN particle hydrogels immediately after polymerization. Inserts in plot are representative images of the PRNHs. Thiol:ene functional groups were 1:1 for all PRNH. Data points correspond to mean values of three independent particle synthesis. Error bars correspond to the standard deviation about the mean.

above 10% w/v were difficult to compress into thin films. Polymerization of the 4PEGN and CY↓KC traps the silica particles within the crosslinked polymer matrix, and preserves the original periodic microstructure.

The PRNH films are then transferred into deionized water to swell the hydrogel polymer matrix to equilibrium, which red shifts their color and enables them to respond to proteolytic cleavage of CY↓KC. The swollen films are stable in neutral deionized water for weeks without effect to the color.

Silica particles of various sizes were synthesized and incorporated into PRNHs to tune their color. Composites containing 15% w/v PEGN and 1.5% w/v CY↓KC with either 178, 205, 241, or 297 nm particles produced PRNH films that diffracted violet, blue, green, and red light, respectively (Figure 1C). The peak wavelength diffracted by the films is proportional to the theoretical distance between the particles in a near closed-pack structure, which agrees with previous reports of angle-independent structurally colored materials.[21] The change in particle size is responsible for the variation in structural color after centrifugation. Larger particles create near close-packed periodic structures with larger center-to-center distance, resulting in an increased wavelength diffracted. The synthesis of silica particles is detailed in the Methods Section.

Particle Surface Charge Dictates Degradation-Directed Assembly

Silica particles in a swollen PRNH respond to proteolytic peptide cleavage by reassembling into a composite with higher particle volume fraction, shorter particle-to-particle spacing, and shorter peak wavelength diffracted. When immersed in a 1 µg/mL α-chymotrypsin solution, the CY↓KC monomers are degraded at the surface and then throughout the bulk as the protease cleaves and diffuses into the network, producing 4PEGN chains with either charged amine or carboxylic acid end-groups. Chymotrypsin cleaves the CY↓KC peptide between the tyrosine (Y) and lysine (K) amino acids.[22] The response time for these materials vary based on the concentration and turnover rate of the protease. We previously demonstrated color change responses with this material between 253 ± 120 to 20 ± 5 minutes with α-chymotrypsin concentrations of 0.5 µg/mL and 100 µg/mL, respectively.[22] Direct degradation was observed throughout the bulk of the material by staining the cleaved peptide bonds using a fluorescamine assay and fluorescent microscopy. The particles must be confined in a structurally colored periodic microstructure before degradation of the polymer network, otherwise the PRNH does not assemble into a SCC after degradation (Figure S2).

We investigated whether electrostatic bonding of the cleaved peptide and 4PEGN to the nanoparticle is necessary for particle assembly after degradation. PRNHs were fabricated with 228 nm silica particles that were surface functionalized with a short linear PEG (PEG-SiO_2) (See Table 1 for particle size and surface charge **characterization**).[23] **T**he PEG-SiO_2 maintained a stable surface charge (ZP = -37.5 mV), the linear PEG covering the silica surface prevents adsorption of the polymer matrix and electrostatic interactions of the cleaved peptide to the particle surface. The PRNH was placed in a 1 mg/mL α-chymotrypsin solution to degrade 70% of the hydrogel crosslinks.[22] After 30 minutes, the polymer matrix was fully degraded and structural color disappeared. The PEG-SiO_2 functionalized nanoparticles did not reassemble into a SCC, but instead resuspended into the surrounding solution (Figure S3). This indicates that during this degradation process, the particles become coated in polymer and cleaved peptide due to adsorption and electrostatic binding, respectively, decreasing the electrostatic repulsion between particles. The decrease in repulsion causes the particles to assemble in a more disordered structure after the 70% crosslinks have been degraded, producing an even more broad diffraction peak.[22]

Table 1 Surface functional groups added to the silica particles, and the resulting charge and size measurements.

Particle Type	Functional Group	Average Zeta Potential [mV]	Average Size [nm]	PDI
SiO_2	No surface modification	-44.8 ± 5	202	0.02
THOPS-SiO_2	3-(trihydroxysilyl)-1-propanesulfonic acid (THOPS)	-59.3 ± 2	205	0.04
AHAPS-SiO_2	N-(6-aminohexyl)aminopropyltrimethoxysilane (AHAPS)	31.6 ± 3	265	0.18
PEG-SiO_2	[hydroxy(polyethyleneoxy)propyl]triethoxysilane, 8-12 EO (PEG-silane)	-37.6 ± 1	228	0.04

Each measurement indicates three unique particle suspensions.

The surface charge of particles in a suspension is essential to the stability of colloidal systems which occurs through electrostatic repulsion. The absence of surface charge causes nanoparticles to irreversibly aggregate.[24] PRNHs with different particle surface charges were fabricated and the role of surface charge on degradation directed assembly was investigated with zeta potential (ZP) measurements. Silica particles were functionalized with either 3-(trihydroxysilyl)-1-propanesulfonic acid (THOPS), or N-(6 aminohexyl)aminopropyltrimethoxysilane (AHAPS) to obtain negative (ZP = -65 mV) or positive (ZP = +32 mV) surface charge (Figure 2). We found that PRNHs that contain either THOPS or AHAPS functionalized particles ($PRNH^-$ and $PRNH^+$) can assemble into a composite with shorter interparticle distances following 70% degradation[22] of the polymer network. However, only the THOPS functionalized $PRNH^-$ degraded into a composite with structural color. The $PRNH^+$ instead degraded into a material that irreversibly aggregated, incoherently diffracted light, and appeared white (Figure S4). This suggests that the AHAPS-SiO_2 particles require a larger surface charge to provide repulsion when the particles assemble after degradation like other positively charged colloids that can assemble into arrays with structural color.[25]

The ZP of silica particle suspensions was measured to determine whether repulsion exists in a completely degraded hydrogel. PRNH$^-$, PRNH$^+$ and PRNH with silica that has no surface modification (SiO$_2$) were fabricated and placed in a α-chymotrypsin solution to completely degrade the polymer network. After complete degradation of the hydrogel, the particles suspended into the surrounding solution, as evident by an increase in the solution turbidity, and those suspensions were tested for their ZP. In neutral deionized water, all particles were stable in solution with zeta potentials above $\pm$30 mV.[26]

When dispersed in Tris buffer, the AHAPS-SiO$_2$ ZP reduces to near zero (- 0.02 mV) due to charge screening by the CaCl$_2$ and Tris salts to the particle surface. The ZP of the SiO$_2$ and THOPS-SiO$_2$ nanoparticles also decreased when placed in Tris buffer to -10.0 and -19.8 mV, respectively. The completely degraded PRNH suspensions had an even smaller ZP of 0.01, -4.1, and -7.3 mV for the AHAPS-silica, SiO$_2$, and THOPS-SiO$_2$, respectively, indicating that the degraded polymer provides additional electrostatic charge neutralization.

Physical bonding of the degraded polymer and cleaved peptide to the particle surface drastically reduces the electrostatic repulsion between particles because of charge neutralization effects. THOPS-SiO$_2$ is the only particle type tested that maintains a negative ZP after immersion in TRIS buffer (-19.8 mV) and after complete degradation of the polymer network (-7.3 mV). PRNH$^-$ is also the only PRNH that can self-assemble into a colored material after degradation. This suggests that strong electrostatic repulsion between the particles is what allows degradation-directed assembly to form a SCC. PRNH$^+$ does not assemble into a SCC after degradation because the particles have no surface charge. Instead, AHAPS-SiO$_2$ aggregate and the PRNH$^+$ becomes disordered on the surface. A PRNH can color change only if fabricated using positively or negatively charged particles with sufficiently strong surface charge.

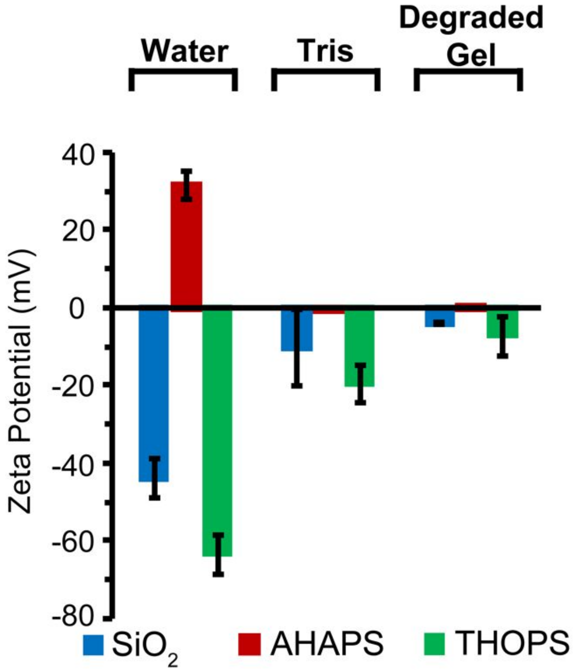

Fig. 2 Functionalized and unfunctionalized SiO$_2$ particles become unstable after complete degradation of the PRNH peptide crosslinks. The zeta potential of silica particles with either THOPS, AHAPS, or no surface chemical functionalization were measured in deionized water, Tris buffer (100 mM) with CaCl$_2$ (10mM), and this Tris buffer with a completely degraded particle hydrogel and α-chymotrypsin (1mg/mL).

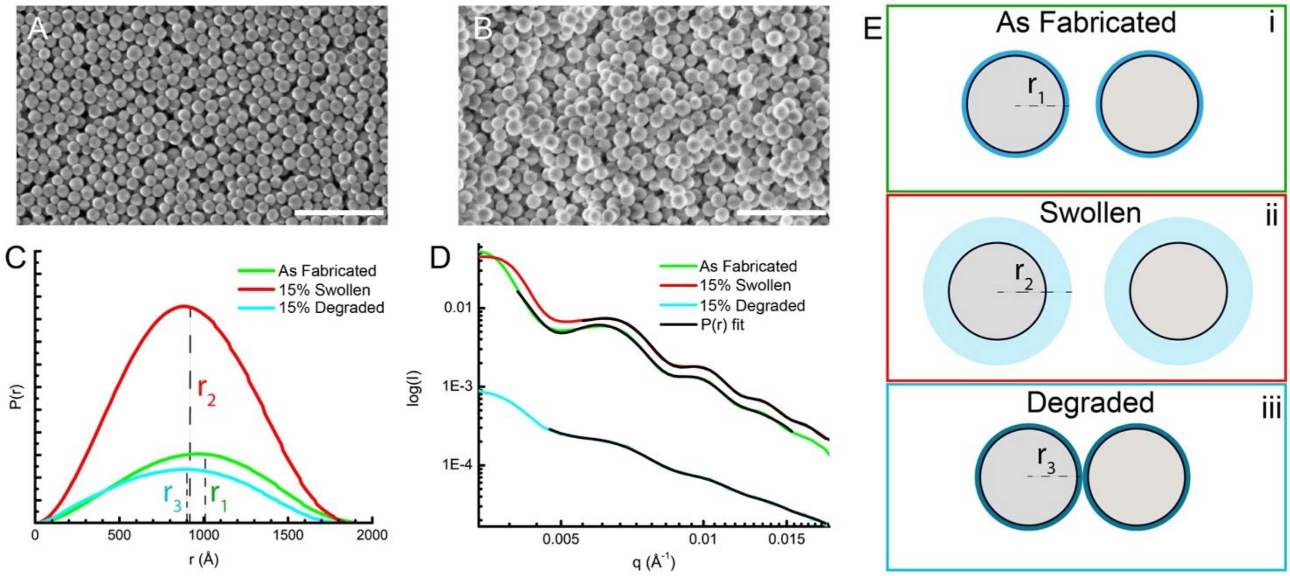

Fig. 3 SEM and USAXS reveals that the degraded PRNH microstructure is less ordered than the initially fabricated state. Scanning electron micrograph of the surface of a dried PRNH (A) after being centrifuged and polymerized, and (B) after degradation-directed assembly. (C) P(r) fit function for (D) USAXS of PRNH as fabricated, swollen, and degraded PRNHs. PRNH with 15% w/v 4PEGN were used with 1:1 thiol:ene functional groups. Scattering intensities were offset vertically for clarity. (E) Schematic representation of the nanoparticle interactions with the peptide and polymer matrix at the immediate vicinity of the particle in the (i) as fabricated, (ii) swollen, and (iii) degraded state. Scale bar = 1 µm

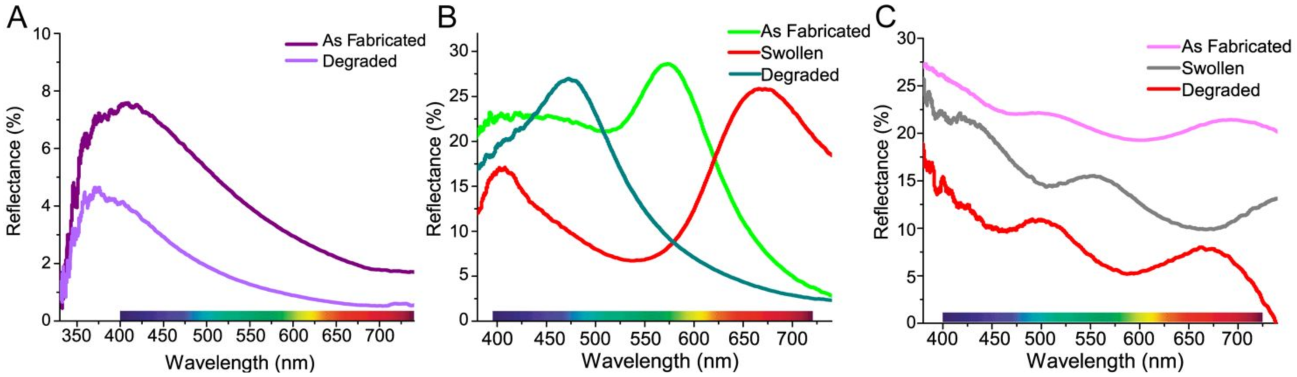

Fig. 4 Altering the particle size does not prevent the degradation-directed assembly of PRNH and yields degraded composites with different structural color. The reflectance measurements of PRNHs with (A) 171 nm, (B) 230 nm, or (C) 313 nm THOPS-SiO_2 in the as fabricated, swollen, and degraded states. The swollen state of the 171 nm silica particle hydrogel measurement was omitted due to lack of reflectance peak in the swollen state. Reflectance measurements were offset vertically for clarity. The reflectance spectra shown are representative data for the experimental samples. n=4.

Observation of Particle Aggregation in Degraded PRNHs

The decrease in electrostatic repulsion that occurs during degradation of the PRNH allows for a controlled aggregation event to occur between the silica particles. We confirmed this hypothesis by performing SEM and USAXS on the PRNH in the initial “as fabricated” state, immediately after centrifugation and polymerization; the “swollen” state, when the PRNH has been immersed and swollen to equilibrium in deionized water; and the “degraded” state, after a 70% of crosslinks have been cleaved by α-chymotrypsin and the PRNH has assembled into a composite with shorter interparticle distances (Figure 3).[27] The SEM micrographs show that the as fabricated PRNH exhibit short-range order after centrifugation (Figure 3A), which is demonstrated by angle-independent structural color. Iridescent color only exists when the periodic structures have long-range order. When the periodicities have short-range order, non-iridescent color is observed.[19,20] The degraded material (Figure 3B), has particles with more visible aggregation, but even shorter interparticle distances than the initially fabricated state. This decrease in spacing explains how the PRNH changes color from the swollen state to the degraded state. The more aggregated structure of the degraded material gives rise to a broader reflectance peak than the initially fabricated material.

Particle hydrogel composites with ordered particle assemblies exhibit sharp x-ray scattering peaks that yield information of structures at the nano- and microscale.[28,29] The scattering pattern of the PRNH would indicate whether the surface microstructure observed in Figure 3A and 3B is uniform throughout the film, and if the particle arrangement changes after degradation. USAXS of the as fabricated, swollen, and degraded PRNHs was performed and the pair-distance distribution function (P(r)) was modeled (Figure 3C) and used to fit to the 1-D scattering obtained (Figure 3D).[30] There is non-interacting polymer and peptide that surround the silica nanoparticles when the material is initially fabricated (Figure 3E) which yields a full width at half maximum (FWHM) of 114 nm centered at 95 nm in the P(r). The polymer and peptide matrix swells when the PRNH is swollen to equilibrium, and the scattering observed is more uniform than the initially fabricated state as indicated by the decrease of the FWHM to 105 nm center at 89 nm. This occurs because there is less polymer and peptide neighboring the particles due to swelling. When the PRNH is degraded, the scattering pattern is dampened due to the aggregation of particles caused by the electrostatic binding of cleaved peptide onto the particle surface producing a FWHM of 126 nm centered at 87 nm. Dampened scattering patterns similar to those produced by the degraded PRNH have been observed before in aggregated particle suspensions,[31] corroborating that aggregation occurs in the bulk of the material after degradation-directed assembly.

The Effect of Particle Size on the PRNH Degradation-Directed Assembly

A unique feature of the PRNH is that the degradable peptide monomer can be substituted for other peptides that would allow for specific protease sensing. By leveraging particle size to create sensors with different responses and variation in structural color, arrays of PRNHs can be made to yield specific optical readout of enzyme presence in solution. To demonstrate this concept, 180, 240, and 300 nm THOPS-SiO_2 were used to create PRNHs with different structural colors. Importantly, the PRNH was investigated at three different states during which it possesses different structural colors and varying degrees of order: as fabricated (after centrifugation and polymerization), swollen, and after being degraded by α-chymotrypsin. The PRNH’s reflectance was characterized during each state using reflectance probe spectroscopy (Figure 4).

For all particle sizes tested, PRNHs self-assembled during degradation into composites with shorter interparticle spacing compared to the non-degraded as fabricated material, causing a discernable change in structural color between the swollen and degraded states. Interestingly, the degraded PRNHs diffracted wavelengths shorter than the as fabricated state. For example, the color of the PRNH containing 171 nm particles shifted from diffracting violet light, 409 nm, in the as fabricated state to UV light, 371 nm in the degraded state

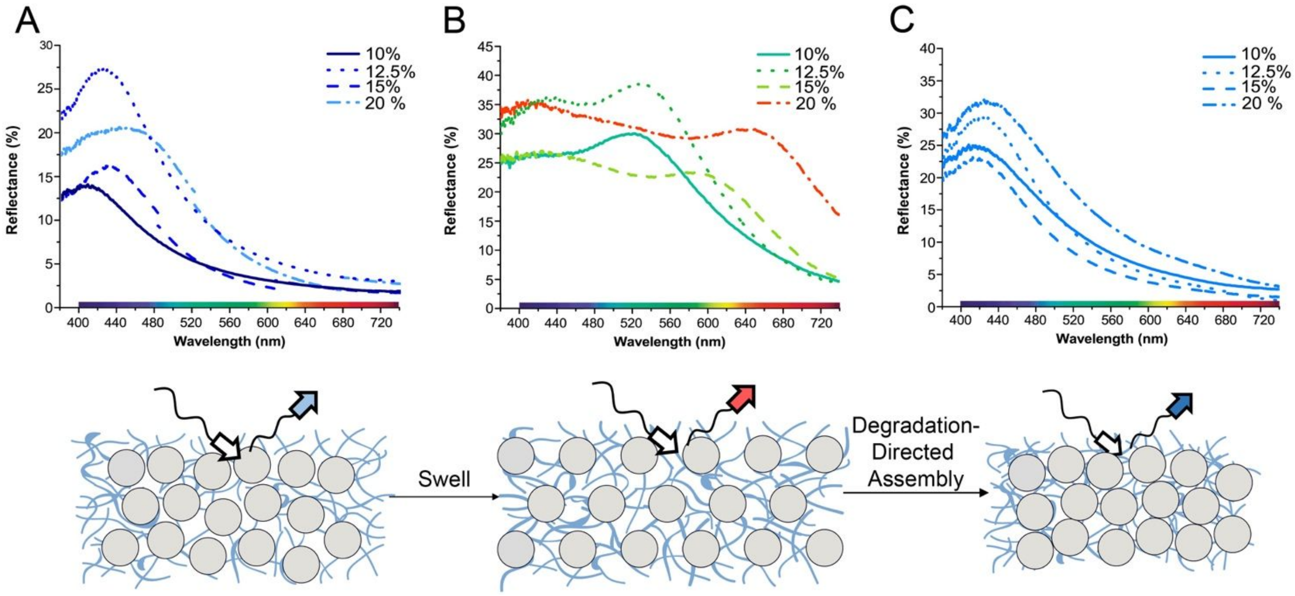

Fig. 5 Altering the polymer concentration of the PRNH does not inhibit the degradation-directed assembly and produces different color changes between the swollen and degraded states. 210 nm THOPS modified silica particles were used to fabricate structurally colored PRNH. Polymer concentrations were varied (10–20 % w/v) to yield different colors in the swollen state. Reflectance spectra were characterized in the (A) as fabricated, (B) swollen, and (C) degraded state. The bottom schematic illustrates the states of the PRNH in the initially fabricated (left), swollen (middle), and reassembled/degraded (right) state. The reflectance spectra shown are representative data for the experimental samples. n = 4

(Figure 4A). This implies that particle assembly produces a PRNH with smaller particle-to-particle distance than the centrifuged as fabricated state. The 240 nm PRNH also demonstrated this behavior, but diffracted green light, 573 nm, in the as fabricated state, red light, 666 nm, in the swollen state, and blue light, 472 nm, in the degraded state (Figure 4B). The PRNH containing 313 nm particles is red in the as fabricated state, diffracting 693 nm light, and diffracts 661 nm light in the degraded state (Figure 4C). The PRNH with 313 nm particles also swells into the infrared region of light, allowing it to be used as a white-to-color sensor. Peaks are also observed in the blue and green region of visible light for the 313 nm particles due to backscattering at those wavelengths.[32]

The Effect of Polymer Concentration on the PRNH Degradation-Directed Assembly

Peptide-polymer adsorption to the silica particles directs self-assembly after degradation but increasing polymer concentration could affect self-assembly by slowing down local diffusion of the silica particles. We examined the effect of initial polymer concentration on degradation-directed nanoparticle assembly using PRNHs fabricated with 205 nm THOPS-SiO_2. Polymer concentrations between 10–20 % (w/v) were used to produce PRNHs that diffracted visible light in the swollen state (Figure 5). Polymer concentrations below or above 10–20 % either did not swell enough to increase the diffracted wavelength compared to the as fabricated state, or the PRNH swelled too much, diffracting light beyond the visible spectrum, respectively. Reflectance spectrum of the PRNH were measured for the as fabricated (Figure 5A), swollen (Figure 5B) and degraded states (Figure 5C).

Increasing polymer concentration influences the center-to-center distance between particles after centrifugation. The as fabricated PRNHs with 205 nm particles were blue, but the peak wavelength diffracted increased as polymer concentration increased, from 409 nm at 10% w/v to 455 nm at 20% w/v. This difference is due to the increased volume occupied by polymer chains in between the particles. The reflectance peak also broadened for the 20% polymer concentration samples (Figure 5A), likely because the polymer and peptide interfered with the particle ordering during centrifugation. In the swollen state, the color of the PRNH increased proportionally to polymer concentration, diffracting 522 nm at 10% w/v and 649 nm at 20% w/v (Figure 5B).

Upon 70% cleavage of the peptide crosslinks, the PRNH reassembled and the peak wavelength diffracted decreased. Interestingly, the degraded 12.5% (425 nm), 15% (418 nm), and 20% (426 nm) samples diffracted shorter wavelengths than the as fabricated PRNH, suggesting that degradation-directed nanoparticle assembly is not affected by increased polymer and peptide concentration in the hydrogel. Only the 10% degraded sample diffracted a slightly greater peak wavelength than its as fabricated state. In addition, the degraded PRNH diffracted peak wavelengths of nearly the same wavelength for all polymer concentrations tested, which indicates that the nanoparticles assembled to an equilibrium distance that is energetically favorable regardless of polymer concentration. The response time for the degradation-directed assembly is dependent on the substrate concentration and inversely proportional to the enzyme concentration.[22] By varying the polymer content in the PRNH, the response time will change proportionally to the CY↓KC concentration.

Conclusions

A protease responsive SCC that produces distinct color shifts due to large changes in interparticle spacing was fabricated and characterized. We found that electrostatic interactions between the cleaved peptide and nanoparticle facilitates the assembly process that causes color change. In addition, high particle surface charge is required during the degradation-directed assembly because it prevents uncontrolled aggregation that causes destructive scattering of visible light. Along with high surface charge, the particles must also be confined to an arrangement with local ordering so that the degraded PRNH can scatter visible light. If the two previous requirements are met, the PRNHs will undergo the degradation-directed assembly. The color of the PRNH can be tuned by changing the polymer concentration and particle size which yields distinct color changes between the swollen and degraded state of the material. Ultimately, the findings of this manuscript define new design criteria for angle-independent and color changing SCC with specificity to proteases.

Methods

Silica particle synthesis and functionalization

Silica particles were formed through a modified Stöber synthesis.[33] In brief, tetraethyl orthosilicate (6 mL) (Sigma) was mixed with ethanol (70 mL) (Pharmco) vigorously for 5 minutes in a glass round bottom flask. In an Erlenmeyer flask, ammonium hydroxide (Sigma) was mixed with deionized water at various concentrations to yield different particle diameters. 1.25, 1.5, 1.75, and 2 mL of ammonium hydroxide were used for obtain the particle sizes shown in Figure 1C. The ammonium hydroxide solution was mixed the TEOS solution at 250 rpm for 2 hours at which point the reaction reached completion. Functionalization of the silica particle surface was performed via a 6 hour reflux reaction with one of the following: 3-(trihydroxysilyl)-1-propanesulfonic acid, N-(6-aminohexyl)aminopropyltrimethoxysilane, or [Hydroxy(polyethyleneoxy)propyl]triethoxysilane (8-12 EO) (1.5 mL) (Gelest, Inc).[23,34]. The particles were washed by centrifuging suspensions then resuspending with deionized water until the pH of the water phase was neutral. Finally, the particles were concentrated to 100 mg/mL and stored with mixed bed ion-exchange resin (200mg) (Bio-rad) until use.

Fabrication of the structurally colored protease responsive nanoparticle hydrogel

First silica particle suspension (300 μL) is centrifuged at 19318 times the gravitational acceleration for 2.5 minutes. The supernatant is removed and the resulting silica nanoparticle pellet diffracts visible light proportional to the diameter of particle used in the fabrication. To prepare the hydrogel precursor solution, 10 kDa 4PEGN (Sigma) and CY↓KC peptide (Genscript) were dissolved in 2-Hydroxy-4′-(2-hydroxyethoxy)-2-methylpropiophenone (100 μL, mg/mL)(Sigma) at a 4PEGN to CY↓KC molar ratio of 1:2. The pelleted silica particles were then suspended in the hydrogel precursor solution. The final mixture is once again centrifuged for the same time and speed. After removing the supernatant, the pellet is sandwich casted between two cover slips (VWR) by hand and polymerized by UV light exposure (KAIS UV oven) for 20 minutes. The thiol groups on the peptide's cysteine residues react with double carbon-carbon –ene bonds on the norbornene group attached to the 4- arm PEG crosslinker via thiol-ene click chemistry under UV exposure. The resulting crosslinked polymer nanoparticle films are placed in water to swell for one hour before use.

Zeta potential measurements of resuspended particles in degraded hydrogel fragments

Bare silica, THOPS silica, and AHAPS silica were characterized for their surface charge using a Malevern Zeta Sizer Nano ZS90 in deionized water, and a solution of calcium chloride (10 mM) and Tris-HCl (100 mM) titrated to pH 8. To test measure the surface charge of the colloid after complete degradation of the hydrogel, PRNHs were prepared and placed in solutions of α-chymotrypsin (1 mg/mL) in calcium chloride (10 mM) and Tris-HCl (100 mM) titrated to pH 8 for 1 hour at 37°C. Aliquots of the degraded PRNH were diluted in TRIS buffer.

USAXS

PRNHs were fabricated as previously mentioned, but compressed and polymerization between two 0.0254 mm mylar films (Chemplex). Hydrated PRNH were characterized at the Advanced Photon Source within Argonne National Labs using the 21 keV X-rays on the USAXS beamline 9-ID.[27] The program ScÅtter was used for pair distance distribution function fitting from ~ 0.005 to 0.015 Å^{-1} using Moore's method.[30]

PRNH color change experiments

PRNHs were submerged in α-chymotrypsin (1 μg/mL) in calcium chloride (10 mM) and Tris-HCl (100 mM) titrated to pH 8 for 3 hours at 37°C to degrade 70% of the hydrogel. After a color change was observed, diffuse reflectance was measured using a Thorlabs CCS100 spectrophotometer equipped with a SLS201 Light Source and RP20 reflection probe, set to 45°. The measured spectrum for each sample was normalized to the maximum reflectance spectrum as measured on an Ocean Optics WS-1 white reflectance standard, and reported as percent reflectance.

Conflicts of interest

There are no conflicts to declare.

Acknowledgements

This material is based upon work supported by the National Science Foundation Graduate Research Fellowship Program (L.T.Jr) under Grant No. DGE132210. Any opinions, findings, and conclusions or recommendations expressed in this material are those of the author(s) and do not necessarily reflect the views of the National

Science Foundation. J.L.D. was supported by the National Institute of Biomedical Imaging and Bioengineering of the National Institutes of Health under Award Number F31EB025735. The content is solely the responsibility of the authors and does not necessarily represent the official views of the National Institutes of Health. HG received support from the UMD ASPIRE program. The authors would like to acknowledge Dr. R. Briber, and Dr. W. Hwang for their useful discussions and feedback. We would like to thank Dr. S. Muro for allowing us to use the Malvern instrument in her laboratory. We also thank the UMD Nanocenter, AIM Laboratory, and Functional Macromolecular Laboratory for their assistance in the microscopy of the PRNH. This research used resources of the Advanced Photon Source, a U.S. Department of Energy (DOE) Office of Science User Facility operated for the DOE Office of Science by Argonne National Laboratory under Contract No. DE-AC02-06CH11357.

Notes and references

1 C. Fenzl, T. Hirsch and O. S. Wolfbeis, Photonic Crystals for Chemical Sensing and Biosensing, *Angewandte Chemie International Edition*, 2014, **53**, 3318–3335.
2 Y. Takeoka, Stimuli-responsive opals: colloidal crystals and colloidal amorphous arrays for use in functional structurally colored materials, *Journal of Materials Chemistry C*, 2013, **1**, 6059.
3 L. Bai, V. C. Mai, Y. Lim, S. Hou, H. Möhwald and H. Duan, Large-Scale Noniridescent Structural Color Printing Enabled by Infiltration-Driven Nonequilibrium Colloidal Assembly, *Advanced Materials*, 2018, **30**, 1705667.
4 Q. Li, Y. Zhang, L. Shi, H. Qiu, S. Zhang, N. Qi, J. Hu, W. Yuan, X. Zhang and K.-Q. Zhang, Additive Mixing and Conformal Coating of Noniridescent Structural Colors with Robust Mechanical Properties Fabricated by Atomization Deposition, *ACS Nano*, 2018, **12**, 3095–3102.
5 M. Qiu, M. Mulot, M. Swillo, S. Anand, B. Jaskorzynska, A. Karlsson, M. Kamp and A. Forchel, Photonic crystal optical filter based on contra-directional waveguide coupling, *Applied Physics Letters*, 2003, **83**, 5121–5123.
6 J. C. Knight, T. A. Birks, P. S. J. Russell and D. M. Atkin, All-silica single-mode optical fiber with photonic crystal cladding, *Optics letters*, 1996, **21**, 1547–1549.
7 R. D. Deegan, O. Bakajin, T. F. Dupont, G. Huber, S. R. Nagel and T. A. Witten, Capillary flow as the cause of ring stains from dried liquid drops, *Nature*, 1997, **389**, 827–829.
8 R. Williams and R. S. Crandall, The structure of crystallized suspensions of polystyrene spheres, *Physics Letters A*, 1974, **48**, 225–226.
9 M. Xiao, Y. Li, M. C. Allen, D. D. Deheyn, X. Yue, J. Zhao, N. C. Gianneschi, M. D. Shawkey and A. Dhinojwala, Bio-Inspired Structural Colors Produced via Self-Assembly of Synthetic Melanin Nanoparticles, *ACS Nano*, 2015, **9**, 5454–5460.
10 K. Chen, Q. Fu, S. Ye and J. Ge, Multicolor Printing Using Electric-Field-Responsive and Photocurable Photonic Crystals, *Advanced Functional Materials*, 2017, **27**, 1702825.
11 S. Shang, Q. Zhang, H. Wang and Y. Li, Fabrication of magnetic field induced structural colored films with tunable colors and its application on security materials, *Journal of Colloid and Interface Science*, 2017, **485**, 18–24.
12 N. Vogel, M. Retsch, C.-A. Fustin, A. del Campo and U. Jonas, Advances in Colloidal Assembly: The Design of Structure and Hierarchy in Two and Three Dimensions, *Chemical Reviews*, 2015, **115**, 6265–6311.
13 P. J. Flory, *Principles of Polymer Chemistry*, Cornell Univeristy Press, 1953.
14 J. Sanders, Colour of Precious Opal, *Nature*, 1964, **204**, 1151–1153.
15 K. I. MacConaghy, C. I. Geary, J. L. Kaar and M. P. Stoykovich, Photonic Crystal Kinase Biosensor, *Journal of the American Chemical Society*, 2014, **136**, 6896–6899.
16 J. Holtz and S. A. Asher, Polymerized colloidal crystal hydrigel films as intelligent chemical sensing materials, *Nature*, 1997, **389**, 827–829.
17 J. D. Joannopoulos, S. G. Johnson, J. N. Winn and R. D. Meade, *Photonic Crystals: Molding the Flow of Light*, Princeton University Press, 2nd edn., 2008.
18 C.-F. Lai, Y.-C. Wang and H.-C. Hsu, High transparency in the structural color resin films through quasi-amorphous arrays of colloidal silica nanospheres, *Journal of Material Chemistry C*, 2016, **4**, 398–406.
19 H. Noh, S. F. Liew, V. Saranathan, S. G. Mochrie, R. O. Prum, E. R. Dufresne and H. Cao, How Noniridescent Colors Are Generated by Quasi-ordered Structures of Bird Feathers, *Advanced Materials*, 2010, **22**, 2871–2880.
20 A. Kawamura, M. Kohri, G. Morimoto, Y. Nannichi, T. Taniguchi and K. Kishikawa, Full-Color Biomimetic Photonic Materials with Iridescent and Non-Iridescent Structural Colors, *Scientific Reports*, , DOI:10.1038/srep33984.
21 Y. Takeoka, M. Honda, T. Seki, M. Ishii and H. Nakamura, Structural Colored Liquid Membrane without Angle Dependence, *ACS Applied Materials & Interfaces*, 2009, **1**, 982–986.
22 O. B. Ayyub and P. Kofinas, Enzyme Induced Stiffening of Nanoparticle–Hydrogel Composites with Structural Color, *ACS Nano*, 2015, **9**, 8004–8011.
23 T. G. Waddell, D. E. Leyden and M. T. DeBello, The nature of organosilane to silica-surface bonding, *Journal of the American Chemical Society*, 1981, **103**, 5303–5307.
24 B. Derjaguin and L. Landau, Theory of the stability of strongly charged lyophobic sols and of the adhesion of strongly charged particles in solutions of electrolytes . URSS 1941, 14, 633., *Acta Physicochimica URSS*, 1941, 633.
25 H. Shim, J. Lim, C. Gyun Shin, S.-J. Jeon, M. Gyu Han and J.-K. Lee, Spectral reflectance switching of colloidal photonic crystal structure composed of positively charged TiO2 nanoparticles, *Applied Physics Letters*, 2012, **100**, 063113.
26 R. J. Hunter, *Foundations of colloid science*, Oxford University Press, 2nd edn., 2001.
27 J. Ilavsky, F. Zhang, R. N. Andrews, I. Kuzmenko, P. R. Jemian, L. E. Levine and A. J. Allen, Development of combined microstructure and structure characterization facility for in situ and operando studies at the Advanced Photon Source, *Journal of Applied Crystallography*, 2018, **51**, 867–882.
28 W. L. Bragg, The structure of some crystals as indicated by their diffraction of x rays, *Proceedings of the Royal Society Mathematical, Physical, and Engineering Sciences*, 1913, **89**, 248–277.
29 E. Marino, T. E. Kodger, G. H. Wegdam and P. Schall, Revealing Driving Forces in Quantum Dot Supercrystal Assembly, *Advanced Materials*, 2018, 1803433.

30 P. B. Moore, Small-angle scattering. Information content and error analysis, *Journal of Applied Crystallography*, 1980, **13**, 168–175.

31 T. Rieker, A. Hanprasopwattana, A. Datye and P. Hubbard, Particle size distribution inferred from small-angle X-ray scattering and transmission electron microscopy, *Langmuir*, 1999, **15**, 638–641.

32 S. Magkiriadou, J.-G. Park, Y.-S. Kim and V. N. Manoharan, Absence of red structural color in photonic glasses, bird feathers, and certain beetles, *Physical Review E*, , DOI:10.1103/PhysRevE.90.062302.

33 W. Stöber and Fink, Controlled growth of monodisperse silica spheres in the micron size range, *Journal of Colloid and Interface Science*, 1968, **26**, 62–69.

34 C. Graf, Q. Gao, I. Schütz, C. N. Noufele, W. Ruan, U. Posselt, E. Korotianskiy, D. Nordmeyer, F. Rancan, S. Hadam, A. Vogt, J. Lademann, V. Haucke and E. Rühl, Surface Functionalization of Silica Nanoparticles Supports Colloidal Stability in Physiological Media and Facilitates Internalization in Cells, *Langmuir*, 2012, **28**, 7598–7613.

Table of Content (ToC) Graphic:

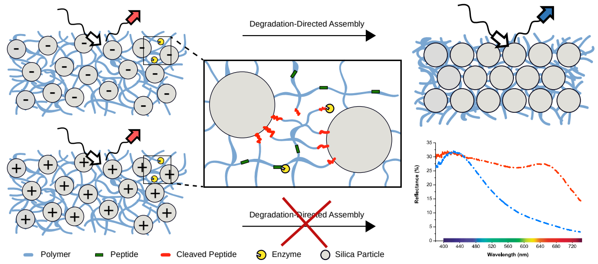

ToC Text: Nanoparticle hydrogels undergo a degradation-directed assembly producing tunable structural color changes for potential sensor applications.